Electronic Supporting Information

Solvent effects leading to different 2D structures in the self-assembly of a crystalline-coil block copolymer with an amphiphilic corona-forming block

Shaofei Song[†], Qing Yu[†], Hang Zhou[†], Garion Hicks[†], Hu Zhu[†], Chandresh Kumar Rastogi[†], Ian Manners[‡], Mitchell A. Winnik*[†§]

[†]Department of Chemistry, University of Toronto, Toronto, Ontario M5S 3H6, Canada

[‡] Department of Chemistry, University of Victoria, Victoria, British Columbia V8W 3V6, Canada

[§]Department of Chemical Engineering and Applied Chemistry, University of Toronto, Toronto, ON M5S 3E2

Corresponding author: mwinnik@chem.utoronto.ca

TABLE OF CONTENTS

1. Additional Experimental Details

1.1 Instrumentation

NMR. ^{1}H NMR (500 MHz) spectra were recorded on an Agilent 500 spectrometer with a 45^o pulse angle and 10 s delay time. The spectra were obtained at 25 ^{o}C in deuterated chloroform ($CDCl_3$). Chemical shifts for ^{1}H NMR were referenced to residual signals from $CHCl_3$ (δ = 7.26 ppm).

Size exclusion chromatography (SEC). SEC measurements were carried out with a Waters 515 HPLC equipped with a Viscotek VE 3580 RI detector, and a 2500 UV-Vis detector. Calibration of the detectors was performed using PMMA standards. THF containing 0.25 g/L tetra-*n*-butylammonium bromide (TBAB) was used as the eluent (flow rate = 0.6 mL/min). The eluent was wormed to 35 ^{o}C.

Transmission electron microscopy (TEM). TEM measurements were performed on a Hitachi D-7000 microscope or a Hitachi HT7700 microscope operating at an accelerating voltage of 80 kV in the bright-field TEM mode. Copper grids from Agar Scientific, mesh 200, were coated with a carbon film. Samples were prepared by placing a drop of solution on the grid and removing excess liquid with the edge of a filter paper. Images were analyzed with the software Image J (NIH, USA). For the statistical analyses, more than 200 micelles in several images were traced by the software in order to obtain the length or other information. The number average micelle length (L_n) and weight average micelle length (L_w) (for 1D cylindrical micelles) or number average micelle long/short axis length (a_n/b_n) and weight average micelle long/short axis length (a_w/b_w) (for 2D platelets) or number average micelle area (A_n) and weight average micelle area (A_w) (for 2D platelets) were calculated as shown below (L, length of object, and also could be referred as long/short axis length; N, number).

$$L_n = \frac{\sum_{i=1}^{n} N_i L_i}{\sum_{i=1}^{n} N_i} \qquad L_w = \frac{\sum_{i=1}^{n} N_i L_i^2}{\sum_{i=1}^{n} N_i L_i} \tag{S1}$$

$$A_n = \frac{\sum_{i=1}^{n} N_i A_i}{\sum_{i=1}^{n} N_i} \qquad A_w = \frac{\sum_{i=1}^{n} N_i A_i^2}{\sum_{i=1}^{n} N_i A_i} \tag{S2}$$

Atomic force microscopy (AFM). Samples for AFM were prepared by drop-casting 8 μL of the micelle solution onto a freshly cleaved mica substrate or carbon-coated copper grid. Height imaging was conducted under ambient conditions using a Bruker Dimension Icon atomic force microscope. All images were obtained with Olympus silicon cantilevers at 320 kHz resonance frequency. Images were analyzed using Gwyddion or Nanoscope Analysis software program.

UV/vis. UV/visible absorbance measurements employed to determine the solution cloud points were performed on a Varian Cary 5000 UV–visible–NIR spectrophotometer equipped with a temperature control device. Wavelengths from 800 nm to 300 nm were recorded. Data employed for cloud point determinations were obtained for λ = 632 nm at different temperatures.[1] The transmitted light was recorded versus temperature, and the cloud point is identified as the temperature at 50% transmittance.

X-ray diffraction (XRD). Power X-ray diffraction measurements were performed on a Rigaku Miniflex 600 diffractometer using Cu Kα (λ = 1.5406 Å) radiation in the 2θ range of 5–60° with a step size of 0.02°. *d*-Spacing is calculated based on Bragg's law $2d \times \sin\theta = n\lambda$. Micelles were prepared on a large scale and then the solution was centrifuged to precipitate the micelles. Collecting the precipitates which was allowed to dry before taking the measurement.

1.2 Materials

All reactions in this work were carried out under N_2 using standard Schlenk line techniques. All chemicals including the inhibitor remover were purchased from Sigma Aldrich and were used as received unless otherwise noted. The monomers (tetradecyl methacrylate (TDMA), oligo(ethylene glycol) methyl ether methacrylate (OEGMA)) used were purified by inhibitor remover to remove the inhibitor (BHT, butylated hydroxytoluene and MEHQ, 4-methoxyphenol). The syntheses and characterization of alkyne-terminated polyferrocenyldimethylsilane (PFS_{27}-alkyne, DP_n = 27) was described in a previous publication.[2] The polymer was characterized by MALDI-TOF with m/z peaks found at 243.0n+260. (The molecular weight of PFS repeat unit is 243.0 Da; the sum of n-butyl and the TMS-aryl-alkyne end groups is 260 Da). M_n^{MALDI} = 6.8 kDa, $Đ$ = 1.03). All the self-assembly experiments were performed in HPLC grade solvents that were acquired from Sigma Aldrich.

2. Synthesis and Characterization of Polymers

Synthesis of P(TDMA-ran-OEGMA)-N_3. This polymer was prepared by atom transfer radical (co)polymerization (ATRP) of TDMA and OEGMA.[3] TDMA (2.4 g, 8.5 mmol), OEGMA (2.55g, 8.5 mmol), CuBr (10 mg, 0.07 mmol), and 2,2'-bipyridyl (BPY) (21.4 mg, 0.14 mmol) were dissolved in toluene (10 mL) in a 25 mL Schlenk tube. After three cycles of freeze-pump-thaw, the azide-functionalized initiator 2-azidoethyl 2-bromoisobutyrate (11.5 μL, 0.07 mmol) was introduced by a

micro syringe to start the polymerization at 80 °C. An aliquot was acquired for monomer OEGMA conversion and total conversion every 0.5 h determination by ^{1}H NMR. The reaction was run for 3.5 h and terminated by cooled using liquid nitrogen and exposure to air. Then the solution was diluted using THF and passed through an aluminum oxide column to remove the residual copper catalyst. After concentrated, it was precipitated by injecting into 50 mL of methanol under vigorous stirring. Using centrifuging, the viscous product was collected. The polymer was subjected to SEC analysis. Monomer conversion: 65 %. ^{1}H NMR ($CDCl_3$, 500 MHz, ppm, Fig. ~~S2~~ S1): δ 4.11 – 4.02 (m, 2H), 3.78 – 3.61 (m, 26H), 3.55 (ddd, *J* = 6.2, 3.2, 1.3 Hz, 3H), 3.38 (q, *J* = 1.8 Hz, 5H), 1.98 – 1.82 (m, 12H), 1.71 – 1.55 (m, 2H), 1.41 – 1.17 (m, 25H), 0.88 (tp, *J* = 7.0, 2.6 Hz, 5H). The monomers can't be completely removed due to the amphiphilic polymers can't be well precipitated in methanol or hexane. SEC (THF/TBAB, RI) (Fig. S2): M_n^{SEC} = 42.7 kD, $Đ$ = 1.27. End-group determination by ^{1}H-NMR was not possible due to signal overlap of initiator and polymer protons.

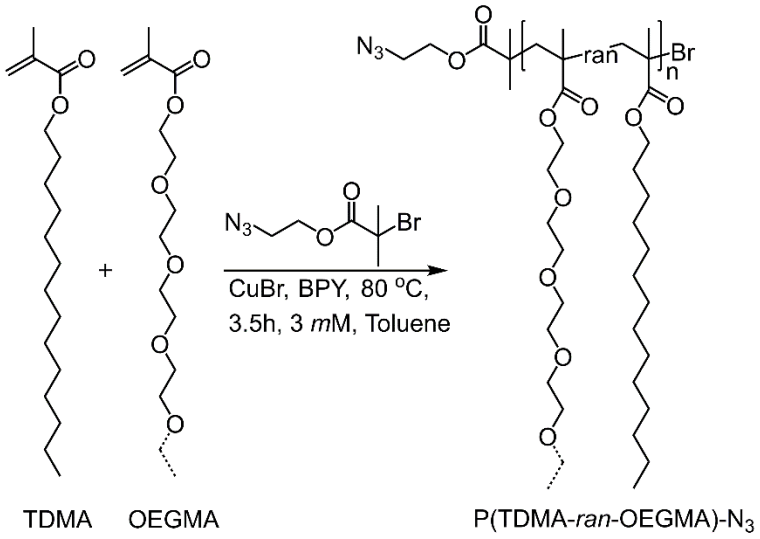

Scheme S1. Synthesis of P(TDMA-*ran*-OEGMA)-N_3 by ATRP.

Reactivity ratios of TDMA and OEGMA. The same polymerization mentioned above was employed to determine the reactivity ratios of TDMA and OEGMA. We used different monomer feed ratios (TDMA/OEGMA = 0:10, 1:9, 2:8, 3:7, 4:6, 5:5, 6:4, 7:3, 8:2, 9:1, 10:0) to study the copolymer composition (*F*) versus monomer feed (*f*) composition and reactivity ratios (*r*). For example, for the 5:5 molar ratio, TDMA (0.6 g, 2.1 mmol), OEGMA (0.63 g, 2.1 mmol), CuBr (2.5 mg, 0.017 mmol), and BPY (5.3 mg, 0.035 mmol) were dissolved in toluene (3 mL) in sealed vials. After three cycles of freeze-pump-thaw, the mixture was heated to 80 °C. The initiator 2-azidoethyl 2-bromoisobutyrate

was diluted in toluene (0.17 mmol/mL), degassed with nitrogen, and then injected by syringe (100 μL, 0.017 mmol) to start the polymerization. To keep the monomer conversion below 20 %, the reaction was run for 30 min and terminated by immersing in liquid nitrogen. An aliquot was acquired for monomer conversion and monomer and copolymer composition determination by ^{1}H NMR. The data were fitted to the Mayo-Lewis equation [4] to determine the reactivity ratios ($r_1 = r^{TDMA}$ and $r_2 = r^{OEGMA}$):

$$r_2 = \frac{f_1}{f_2}\left[\frac{F_2}{F_1}\left(1 + \frac{f_1 r_1}{f_2}\right) - 1\right] \quad \text{(S3)}$$

where f_1 and f_2 are mole fraction of monomers TDMA and OEGMA, and F_1 and F_2 are mole fraction of each monomer in the copolymer. In this way, we calculate values of $r^{TDMA} = 0.99 \pm 0.10$, $r^{OEGMA} = 0.98 \pm 0.12$. Therefore, we conclude that these hydrophobic and hydrophilic units were randomly distributed along the polymer backbone. A plot of copolymer *vs* monomer (TDMA) feed composition for copolymerization of TDMA with OEGMA is shown in Fig. S2c.

Synthesis of PFS$_{27}$-b-P(TDMA-ran-OEGMA). The diblock copolymer PFS$_{27}$-*b*-P(TDMA-*ran*-OEGMA) was prepared via Cu-catalyzed alkyne-azide cycloaddition (CuAAC) reaction between alkyne-terminated PFS$_{27}$-alkyne and P(TDMA-*ran*-OEGMA)-N$_3$ (Scheme 1). PFS$_{27}$-alkyne (50 mg, 7.65 μmol), P(TDMA-*ran*-OEGMA)-N$_3$ (627.5 mg), and PMDETA (16 μL, 76.5 μmol) were dissolved in THF (6 mL) in a Schlenk tube. After three cycles of freeze-pump-thaw, CuCl (7.6 mg, 76.5 μmol) was added. Then the reaction was allowed to stir at 50 ^{o}C for 2 days before being quenched by exposure to air. Aliquots of the mixture were removed before and after the reaction to monitor the reaction progress by SEC. The solution was then diluted with THF and passed through basic Al_2O_3 column to remove the residual copper catalyst.

As indicated in the SEC curves after reaction (Fig. S3), the block copolymers contained small amounts of unreacted PFS homopolymer and P(TDMA-*ran*-OEGMA) copolymer. To purify the BCP, the crude product was first centrifuged at 4000 rpm in THF to remove any undissolved residues followed by slow addition of methanol until a brick red precipitate was observed. Centrifugation to isolate the sediment and repeat of the process removed most of the residual PFS homopolymer, and then washing two times with methanol to eliminate most of the P(TDMA-*ran*-OEGMA) copolymer. After drying, we obtained the BCP (60 mg, yield 30%). The polymer was analyzed by SEC and ^{1}H NMR as following.

The coupling reaction was monitored by SEC with both RI and UV-Vis detectors over the reaction and post-processing. From the SEC curves (Fig. S3), clear peak shifts could be identified from both signals, indicating the successful coupling of two polymers. From SEC-UV curves, no PFS homopolymer left in the BCP sample after purification. ^{1}H-NMR spectrum peak integrations of the purified di-block copolymer in $CDCl_3$ was used to calculate the degree of polymerization (DP) of P(TDMA-*ran*-OEGMA). By comparing the integration of peaks from the Cp rings on PFS and the methylene groups on P(TDMA-*ran*-OEGMA), we calculate a block ratio of around 4.95. Using the PFS signal (DP = 27) as a reference, we calculated DP = 134 for P(TDMA-*ran*-OEGMA) with 65 TDMA units and 69 OEGMA units. Thus, the diblock copolymer is denoted as PFS_{27}-*b*-P($TDMA_{65}$-*ran*-$OEGMA_{69}$)..

^{1}H NMR ($CDCl_3$, 500 MHz, Fig. S4): δ (ppm, integrated peak areas reported are based on Cp protons (4H, Cp) as the reference) = 0.45 (s, 6H, -Si(CH_3)$_2$-Cp, integration = 6.02), 0.78-2.13 (broad, 37H, polymer backbone and side chain of TDMA units), 3.38 (s, 3H, O-CH_3, integration = 7.68), 3.50-3.82 (m, 19H for OEGMA, O-CH_2-CH_2-O, integration = 40.90), 4.00 (s, 4H, Cp, integration = 4.02), 3.83-3.98(broad, 2H, $COOCH_2$, integration = 3.30), 4.04-4.14 (broad, 2H, $COOCH_2$, integration = 4.15), 4.21 (s, 4H, Cp, integration = 4.00). SEC (THF/TBAB, RI): M_n^{SEC} = 52.9 kDa, $Đ$ = 1.17.

Synthesis of PTDMA and POEGMA homopolymers. Each homopolymer was prepared by reversible addition−fragmentation chain-transfer (RAFT) polymerization of tetradecyl methacrylate (TDMA) and oligo(ethylene glycol) methyl ether methacrylate (OEGMA), respectively, as shown in Scheme S2.[5] For instance, TDMA (5.1 g, 18 mmol), AIBN (4.92 mg, 0.03 mmol), and RAFT agent 3-azidopropyl 4-cyano-4-((phenylcarbonothioyl)thio) pentanoate (41.9 mg, 0.15 mmol) were dissolved in 1,4-dioxane (15 mL) in a 25 mL Schlenk tube. After three cycles of freeze-pump-thaw, the Schlenk tube was transferred into the oil pot to start the polymerization at 80 °C. The reaction was run for 8 h and terminated by cooled using liquid nitrogen and exposure to air. An aliquot was removed for monomer conversion determination by ^{1}H NMR. Then the solution was precipitated by injecting into 50 mL of methanol under vigorous stirring. Using centrifuging, the viscous product was washed and collected. The polymer was subjected to SEC analysis. Monomer conversion: 70 %. ^{1}H NMR ($CDCl_3$, 500 MHz, ppm): δ 3.83 – 4.00 (m, 2H), 1.69– 2.09 (m, 3H), 1.57 (s, 2H), 1.27 (s, 26H), 0.87 (tp, J = 9.1, 7.9, 2.6 Hz, 3H). SEC (THF/TBAB, RI): M_n^{SEC} = 38.9 kD, $Đ$ = 1.21. End-group determination by

^{1}H-NMR was not possible due to signal overlap of initiator and polymer protons.

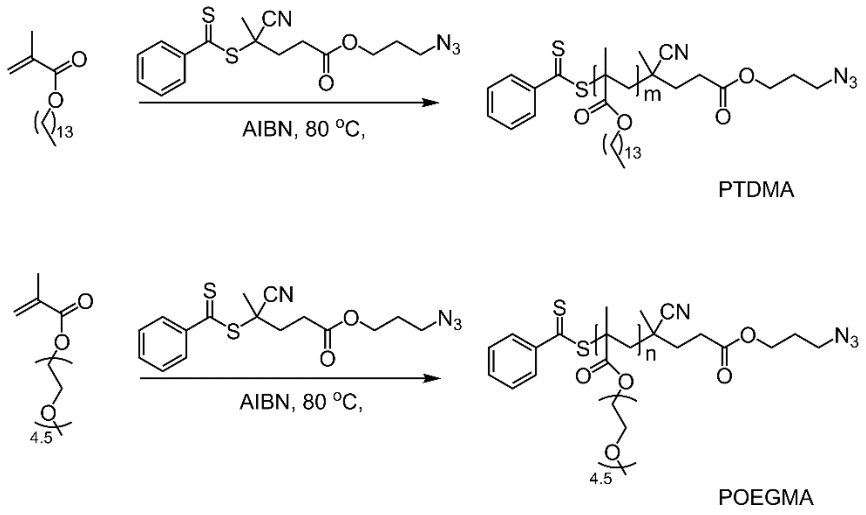

Scheme S2. Synthesis of PTDMA and POEGMA homopolymers by RAFT.

POEGMA homopolymer was prepared using the same procedures for PTDMA. ^{1}H NMR ($CDCl_3$, 500 MHz, ppm): δ 4.15 – 3.99 (m, 2H), 3.71 – 3.58 (m, 14H), 3.58-3.51 (m, 2H), 3.37 (s, 3H), 1.81 (s, 2H). SEC (THF/TBAB, RI): M_n^{SEC} = 40.1 kD, $Đ$ = 1.19.

3. Self-assembly experiments

Additional details for some of the self-assembly experiments are provided here.

Seeded growth and self-seeding in iPrOH. Long fiber-like micelles of PFS_{27}-*b*-P($TDMA_{65}$-*ran*-$OEGMA_{69}$) in iPrOH were prepared by the direct assembly approach. Samples of the block copolymer (BCP) and solvent were mixed at a concentration of 0.5 mg/mL in a 4-mL vial. The sealed vials were placed in a hot oil bath at 80 °C for 1 h, followed by slow cooling in which the block was left to cool to room temperature (RT, 23 °C) (over ca. 2.5 h). Subsequently, the solutions were allowed to age for 24 h. Fig. S5 and S6 shows TEM images of the long micelles at different magnifications.

For seeded growth experiments, micelle fragment solutions (0.5 mg/mL) were obtained from long micelles subjected to sonication (70-watt ultrasonic cleaning bath, 30 min at 23 °C). These seed solutions were then diluted with iPrOH to 50 μg/mL, and 1 mL samples were transferred to new vials. Aliquots of PFS_{27}-*b*-P($TDMA_{65}$-*ran*-$OEGMA_{69}$) unimer in THF (10 mg/mL) were added into each vial at a predetermined weight ratio m_{unimer}/m_{seed} and swirled for 10 seconds. Each solution was allowed

to age in the dark for 7 days.

For self-seeding experiments, micelle fragments (0.5 mg/mL) were obtained by sonication from long micelles as described above and then diluted with iPrOH to 50 μg/mL. Samples (1 mL) were transferred to new vials, and then each vial was immersed into an oil bath at a preset temperature. After heating for 30 min, the vial was removed from the oil bath and allowed to cool in air. Subsequently, the solutions were allowed to age for 24 h.

Direct self-assembly experiments. Direct self-assembly experiments were carried out by suspending a known weight (typically 0.5 mg) of BCP in 1 mL of solvent, immersing the vial in an oil bath at 80 °C (sometimes lower temperatures as indicated in the text) for 1 h and allowing the solution to cool slowly to room temperature (RT, 23 °C). We often refer to this protocol as the direct self-assembly approach.

Self-seeding experiments in hexanol. A sample of the biomorphic micelles obtained in hexanol at 0.5 mg/mL was sonicated as described above. This led to mixed fragments of different sizes. Aliquots were diluted with hexanol to 50 μg/mL, and 1 mL samples were heated in an oil bath as described above and cooled to RT.

Self-seeding and seeded growth in 1:1 octane/hexanol. Oval micelles of PFS_{27}-*b*-P($TDMA_{65}$-*ran*-$OEGMA_{69}$) in 1:1 octane/hexanol were prepared at 0.5 mg/mL by the direct assembly approach. Part of this sample was subjected to an identical sonication protocol as the sample in iPrOH. These micelle fragments, which were polydisperse in size, were then diluted with 1:1 octane/hexanol to 50 μg/mL. For self-seeding experiments, 1 mL samples were placed in several vials, and then each vial was immersed into an oil bath at a preset temperature. After heating for 30 min, the vial was removed from the oil bath and allowed to cool in air. Subsequently, the solutions were allowed to age for 24 h.

Seeded growth experiments were carried out in two different ways. One set of experiments employed the micelle fragment solution described in the previous paragraph. Aliquots of PFS_{27}-*b*-P($TDMA_{65}$-*ran*-$OEGMA_{69}$) unimer in THF (10 mg/mL) were added into each vial at a predetermined weight ratio m_{unimer}/m_{seed} and swirled for 10 seconds. Each solution was allowed to age in the dark for 7 days. In the second set of experiment, samples of the intact oval micelles obtained by direct self-assembly at 0.5 mg/mL and 80 °C were diluted with 1:1 (v/v) octane/hexanol to 50 μg/mL. Samples (1 mL) were placed in several vials, and then aliquots of unimer in THF (10 mg/mL) were added into

each vial at a predetermined weight ratio m_{unimer}/m_{seed}. The samples were aged at RT as described above.

4. Additional Results and Discussion

Self-seeding in hexanol

The micelles formed by direct self-assembly in hexanol comprised ovals that appeared to be grafted to fibers. Sonication of the micelles led to a mixed morphology (Fig. S10a) consisting of short fibers and ill-defined broader objects. When these fragments were subjected to self-seeding at 70 °C, we obtained a mixture of long (ca 2 μm) lenticular micelles with branches of fiber-like micelles protruding from both tips, accompanied by much smaller polydisperse rounded platelets (Fig. S10b).

Self-seeding and seeded growth in 1:1 octane/hexanol

Oval micelles generated by direct self-assembly in 1:1 octane/hexanol were subjected to sonication to yield polydisperse planar structures shown in the TEM images in Fig. S20. These are no longer ovals but are better described as ill-formed clusters. Self-seeding experiments with these fragments at 50 μg/mL led to relatively uniform oval micelles (Fig. S21) at much lower concentration than we could use for direct self-assembly. Seeded growth experiments (Fig. S22) gave a mixed morphology consisting of polydisperse ovals plus some smaller fiber-like structures.

A second set of seeded growth experiments involved addition of unimer in THF (10 mg/mL) to a diluted suspension of the oval micelles generated by direct self-assembly. These experiments were more successful in that larger uniform oval micelles formed (Fig. 8 and S23), and their area increased in proportion to the amount of unimer added (Fig. 8f, main text).

The presence of dark spherical objects and/or occlusions

A reviewer asked us to comment on the dark objects and occlusions that appear in a few images (Fig. 4a,b, S15c, S17a,i, S21c, S22, S23). In some cases, they may be due to dust or problems with sample preparation. We were most concerned with the small dark objects in the TEM images that were found outside the rectangular platelets formed in octane. Here we used selective sedimentation to remove these small dark objects. More difficult to explain are the dark occlusions seen in or on some of the planar structures, particularly the ovals. While most of these objects appear circular in 2D TEM images and may be spherical, they are polydisperse in size. The occlusions have dimensions ranging from 50-150 nm in Fig. S17a,i, 20±10 nm in Fig. S21c, to 70-100 nm in Fig. S22. At his point in time, we have no clear explanation for their nature (amorphous, crystalline) or how they were formed.

5. Supporting Figures

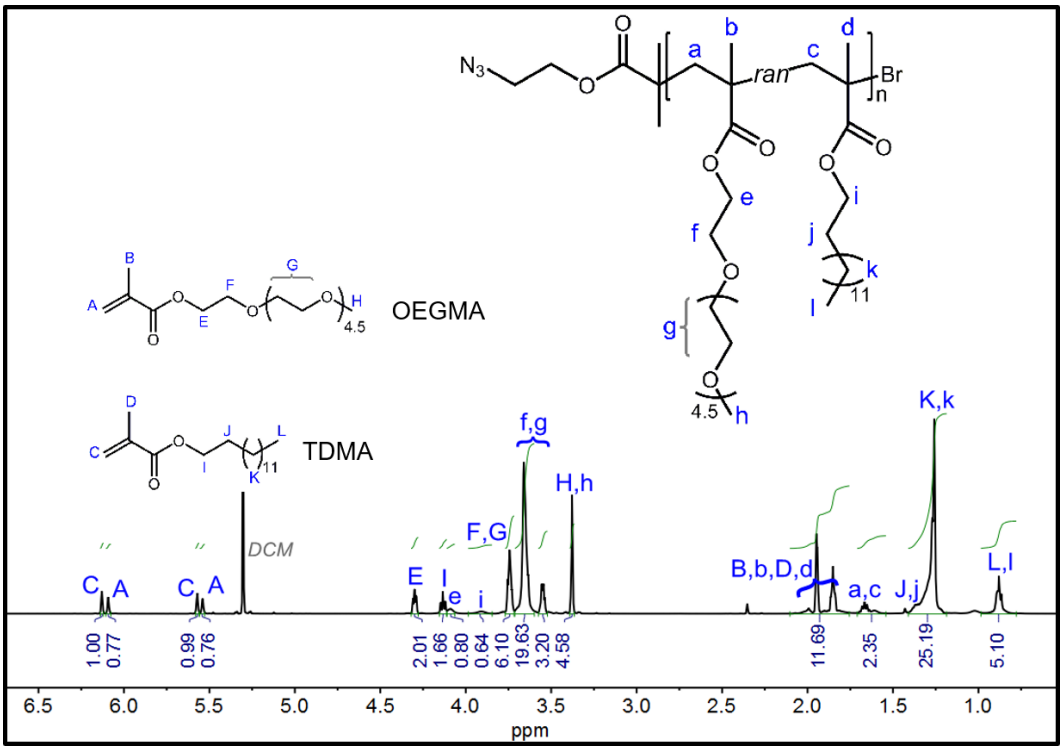

Fig. S1. ^{1}H NMR spectrum of P(TDMA-*ran*-OEGMA)-N_3. After purification using a silica column and precipitation, there was still unreacted monomer remaining. These monomers were removed after coupling to PFS_{27}-C≡CH. Nevertheless, this spectrum enabled calculation of the copolymer composition. Comparing the integration values of the signals from the double bonds (A/C) and the terminal methyl groups of the side chains (H/h and L/l) gave a ratio of 1: 1.06 for TDMA and OEGMA units.

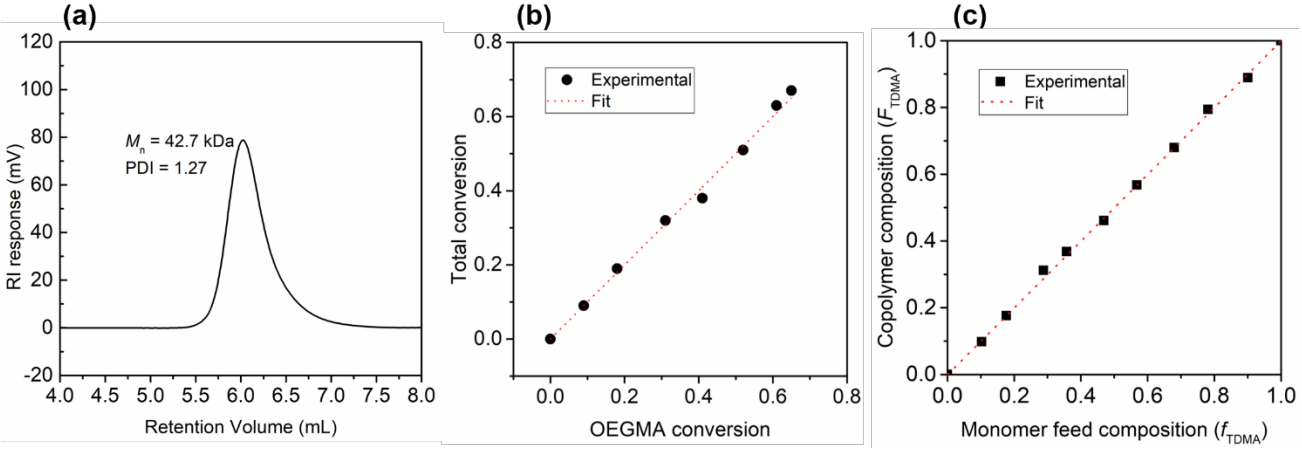

Fig. S2. (a) SEC curve of P(TDMA-*ran*-OEGMA)-N_3 with THF/TBAB as the eluent. The value of DP_n of this random copolymer was determined by ^{1}H NMR after coupling with PFS_{27}-C≡CH. (b) Total polymerization conversion plotted against monomer conversion. The monomer feed ratio TDMA/OEGMA = 1:1 was employed in this study. (c) Copolymer *vs* monomer (TDMA) feed composition for copolymerization of OEGMA with TDMA in toluene solution at 80 °C.

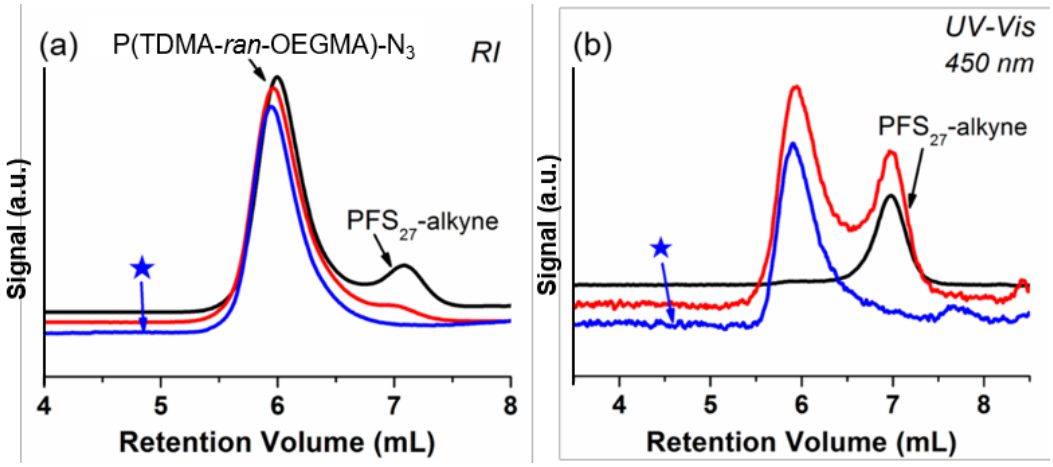

Fig. S3. SEC curves in THF containing TBAB before (black lines) and after (red lines) the click coupling reaction of PFS-alkyne and P(TDMA-*ran*-OEGMA)-N_3 and after purification of the BCP (blue lines). (a) RI signal and (b) UV-Vis signal (UV-Vis detector wavelength: 450 nm). After coupling reaction, the BCP contained small amounts of unreacted PFS homopolymer and P(TDMA-*ran*-OEGMA) copolymer (red lines). To purify the BCP, the crude product was first centrifuged at 4000 rpm in THF to remove any undissolved residues followed by slow addition of methanol until a brick red precipitate was observed. Centrifugation to isolate the sediment and repeat of the process removed most of the residual PFS homopolymer, and then washing two times with methanol to eliminate most of the P(TDMA-*ran*-OEGMA) copolymer. After drying, pure BCP was obtained as indicated by the blue lines in the SEC trace (the blue star refers to the BCP). SEC (THF/TBAB, RI): M_n^{SEC} = 52.9 kDa, $Đ$ = 1.17.

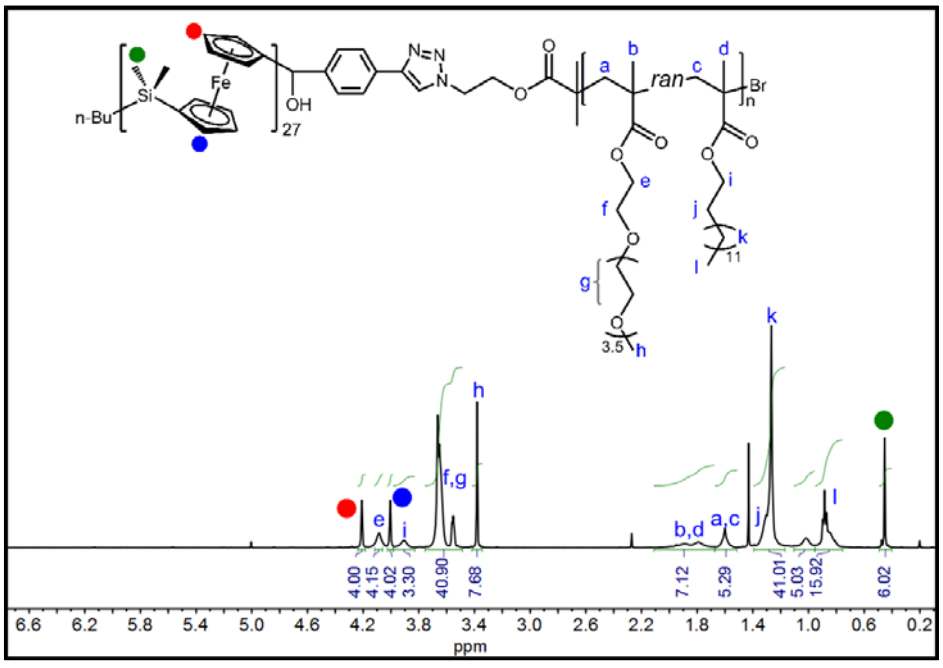

Fig. S4. ^{1}H NMR spectrum of PFS_{27}-*b*-P($TDMA_{65}$-*ran*-$OEGMA_{69}$). Because DP_n of the PFS-alkyne is known from MALDI measurements, its proton signals in the ^{1}H NMR spectrum serve as a reference for determination of DP_n for the block copolymer. Comparing the ferrocene proton signals (●/●) with those of the terminal methyl groups of the side chains (h) gave a ratio of 1:4.95 for the sum of TDMA and OEGMA units, therefore, the DP_n is 134 with 65 TDMA units and 69 OEGMA units.

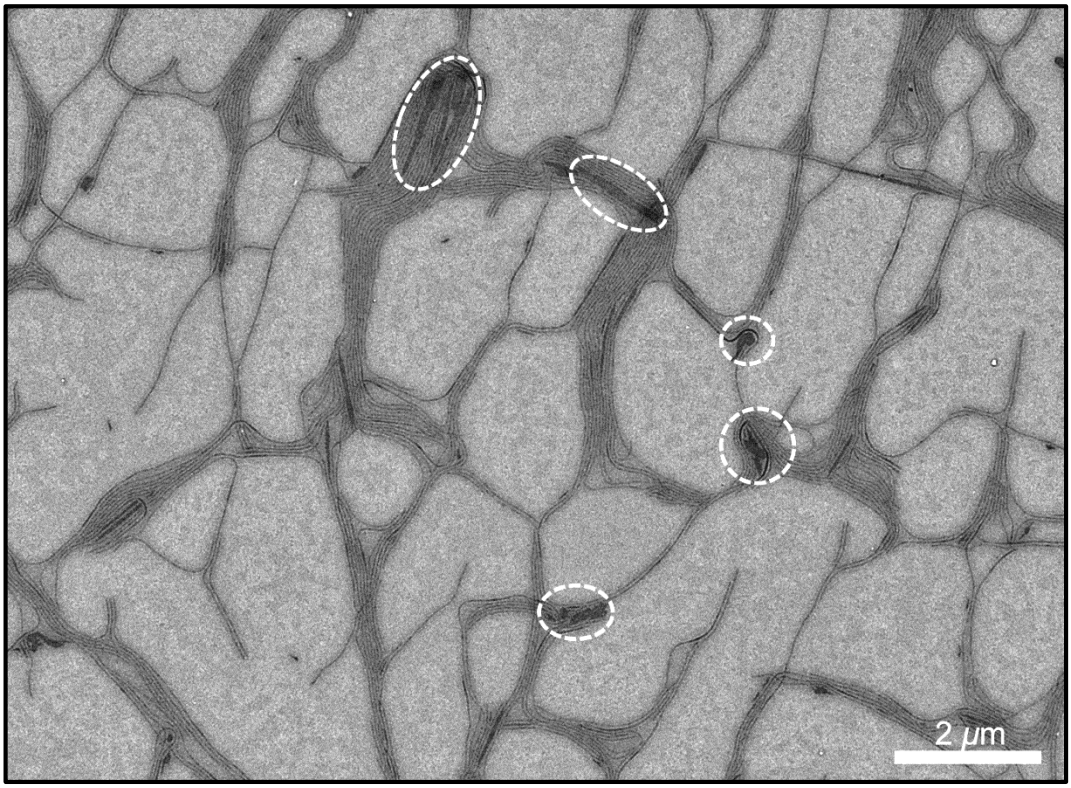

Fig. S5. Long micelles of PFS_{27}-*b*-P($TDMA_{65}$-*ran*-$OEGMA_{69}$) formed by direct self-assembly in iPrOH (0.5 mg/mL). Note that in addition to the long fiber-like micelles, some platelet-like structures can be seen. These are indicated by the dashed white circles and ellipses. Scale bar 2 *μ*m.

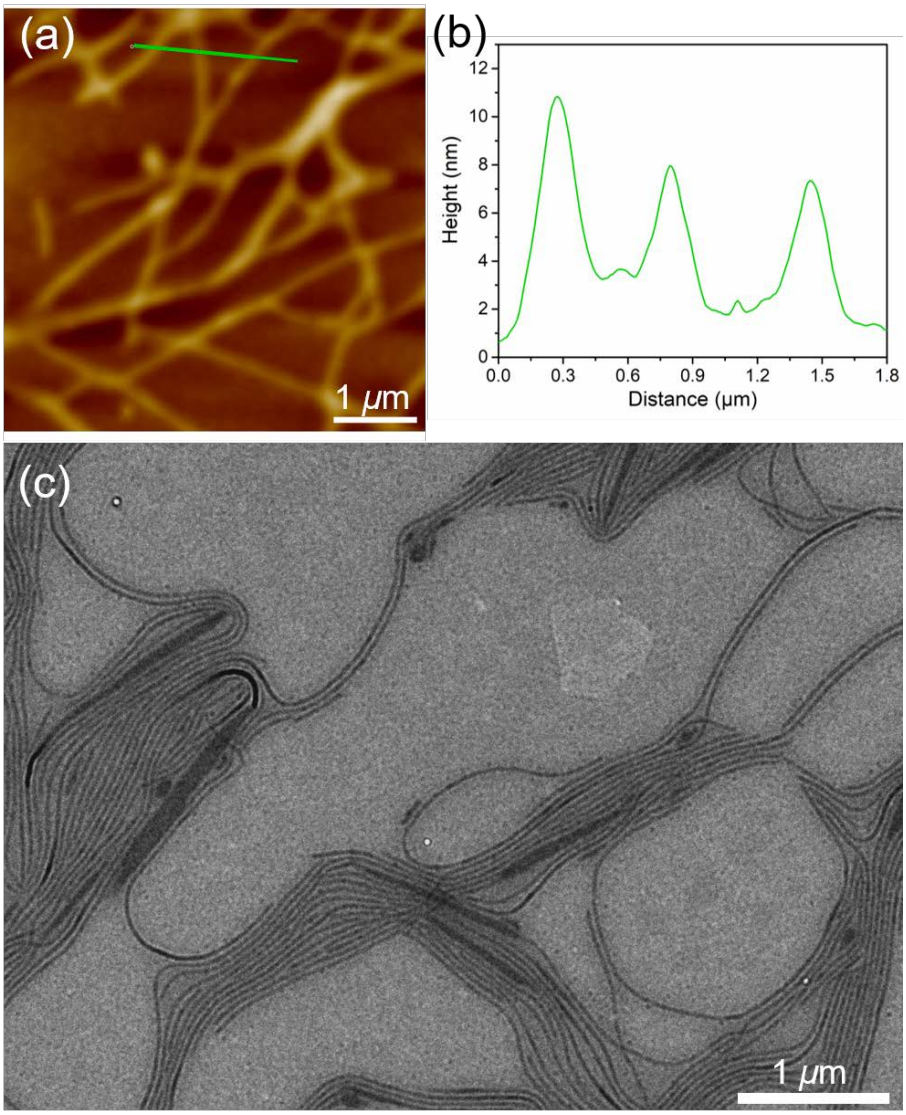

Fig. S6. (a) AFM height image and (b) height profiles of long fiber-like cylindrical micelles formed by PFS_{27}-*b*-P($TDMA_{65}$-*ran*-$OEGMA_{69}$) in iPrOH. These micelles showed a mean height of H_n = 6.5 nm, H_w = 6.9 nm, H_w/H_n = 1.06, determined by measuring 50 sites in this image. The peak in (b) with a height of 11 nm may point to a twist in the ribbon-like structure. (c) TEM image of the same micelle sample. We used ImageJ to measure the widths of the micelles at 200 positions of the well resolved fiber-like structures [W_n = 30 nm, W_w = 31 nm, W_w/W_n = 1.03].

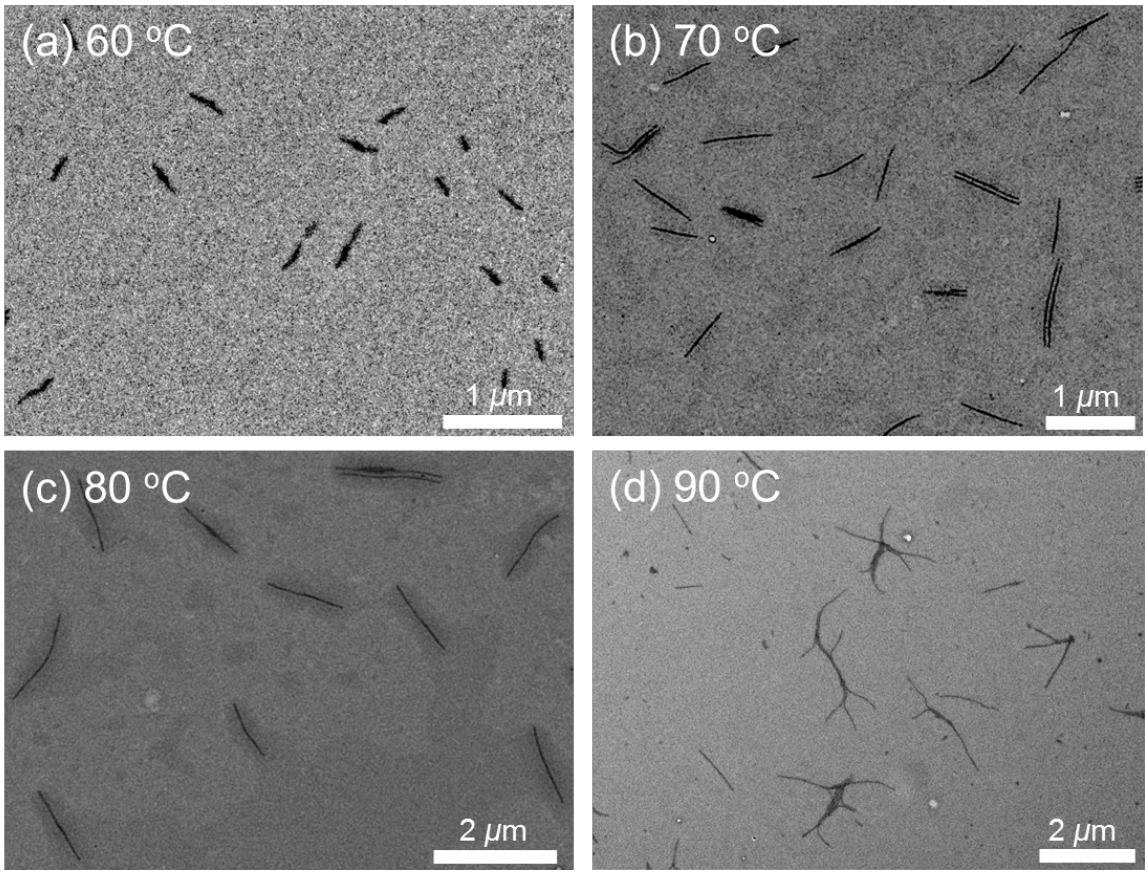

Fig. S7. Self-seeding of PFS_{27}-*b*-P($TDMA_{65}$-*ran*-$OEGMA_{69}$) at different annealing temperature for 30 min in iPrOH. (a) 60 °C, scale bar 1 *μ*m. L_n = 236 nm, L_w = 249 nm, L_w/L_n = 1.05. (b) 70 °C, scale bar 1 *μ*m. L_n = 661 nm, L_w = 669 nm, L_w/L_n = 1.01. (c) 80 °C, scale bar 2 *μ*m. L_n = 1208 nm, L_w = 1225 nm, L_w/L_n = 1.01. (d) 90 °C, scale bar 2 *μ*m. Note that branched structures are formed from samples heated to 90 °C.

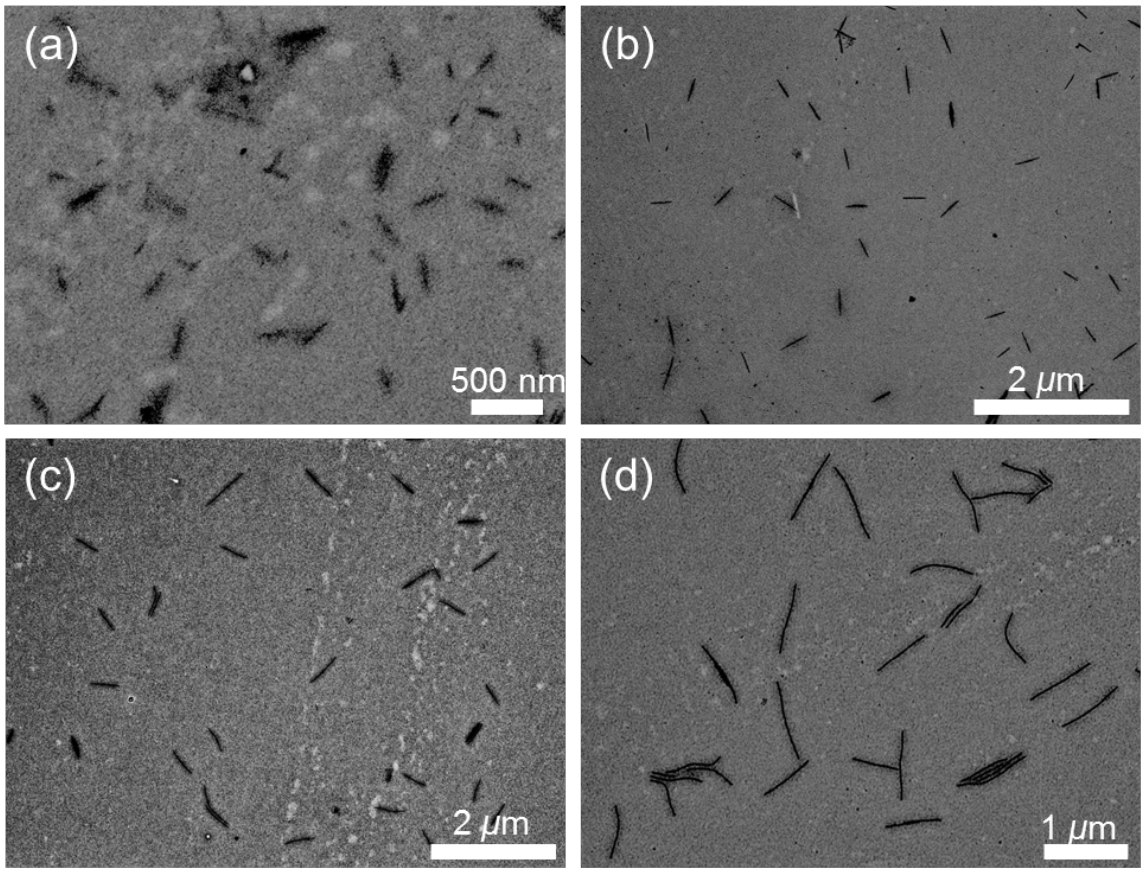

Fig. S8. Seeded growth of PFS_{27}-*b*-P($TDMA_{65}$-*ran*-$OEGMA_{69}$) in iPrOH at different m_{unimer}/m_{seed} ratios. The seed concentration was 0.05 mg/mL. The experiments were conducted at RT and then allowed to age for 7 d, prior to preparing TEM grids. Unimers in THF at 10 mg/mL. (a) 2 eq., scale bar 500 nm. L_n = 167 nm, L_w = 172 nm, L_w/L_n = 1.03. (b) 4 eq., scale bar 2 μm. L_n = 240 nm, L_w = 245 nm, L_w/L_n = 1.02. (c) 8 eq., scale bar 2 μm. L_n = 451 nm, L_w = 484 nm, L_w/L_n = 1.07. (d) 14 eq., scale bar 1 μm. L_n = 753 nm, L_w = 771 nm, L_w/L_n = 1.02. A plot of the number-average length L_n versus m_{unimer}/m_{seeds} for the micelles shown in parts a−d is presented in Fig. 2g of the main text. The dashed line in that plot represents the predicted lengths assuming that all added unimers added to the seed micelles.

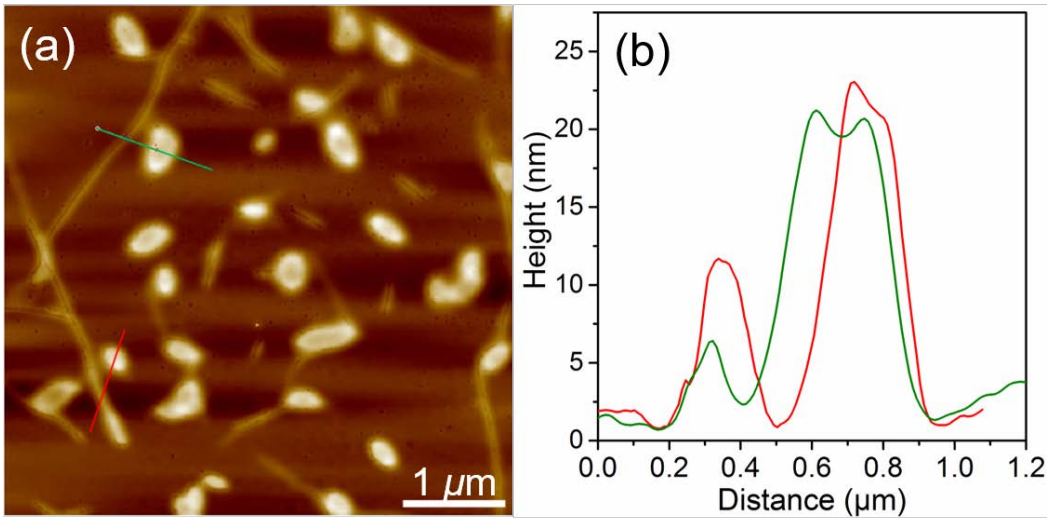

Fig. S9. Micelles formed by self-assembly of PFS_{27}-*b*-P($TDMA_{65}$-*ran*-$OEGMA_{69}$) in 1-hexanol (0.5 mg/mL, 80 °C). (a) AFM image and (b) height profile of the fiber-like structures and oval-like petals. The height of fiber-like micelles was typically ca. 6.5 nm similar to that seen for micelles prepared in 2-propanol. The height of the oval structures (ca. 20 nm) is close to that of the well-defined oval structures formed in 1:1 (v/v) octane/hexanol.

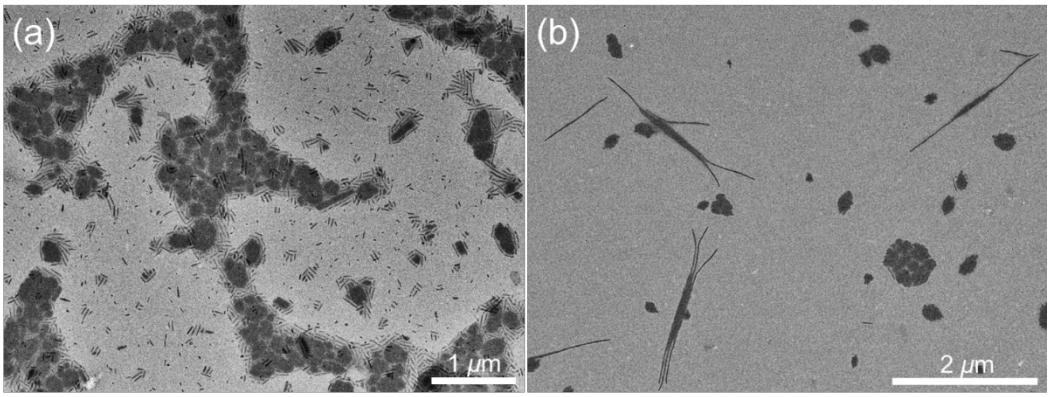

Fig. S10. Self-seeding of PFS_{27}-*b*-P($TDMA_{65}$-*ran*-$OEGMA_{69}$) in 1-hexanol. (a) Seeds from sonication (RT, 30 min), 0.5 mg/mL. Scale bar 1 μm. (b) Micelles (0.05 mg/mL) after self-seeding at 70 °C for 30 min followed by rapid cooling to RT, and then aged for 24 h. However, this process results in a mixture of branched micelles and ovals that are not uniform in size. Scale bar 2 μm.

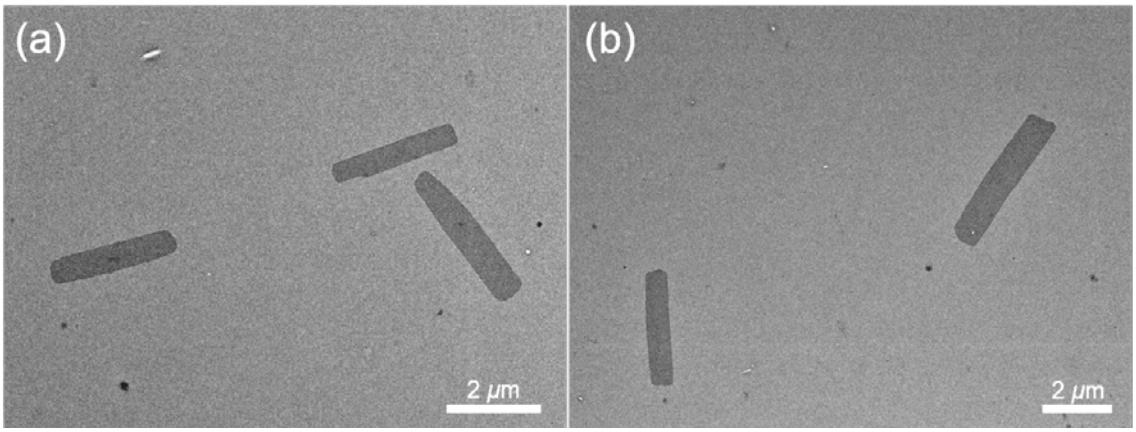

Fig. S11. PFS_{27}-*b*-P($TDMA_{65}$-*ran*-$OEGMA_{69}$) micelles formed by self-assembly in decane (0.5 mg/mL) by heating at 80 °C for 1 h, then slow cooling to RT and aging for 24 h. These platelet micelles showed a mean length of L_n = 3780 nm, L_w = 3860 nm, L_w/L_n = 1.02, and a mean width of W_n = 860 nm, W_w = 890 nm, W_w/W_n = 1.03, determined by measuring 19 samples in five images. Scale bars are 2 μm. Dark spots/occlusions may be dust picked up during transfer of samples or drop-casting them onto the TEM grids.

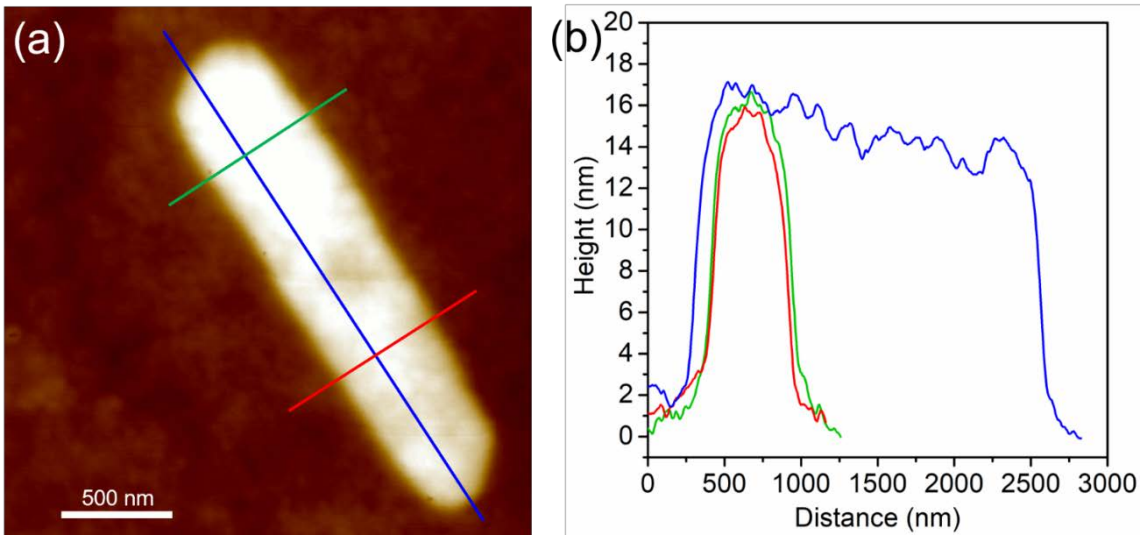

Fig. S12. (a) AFM image and (b) height profile of a rectangular platelet micelles (Fig. 4) formed in octane (0.5 mg/mL) by heating at 80 °C for 1 h, then aged at RT for 24 h). The height of this platelet was uniform (ca. 15 nm) as determined by measuring more than ten positions in this image.

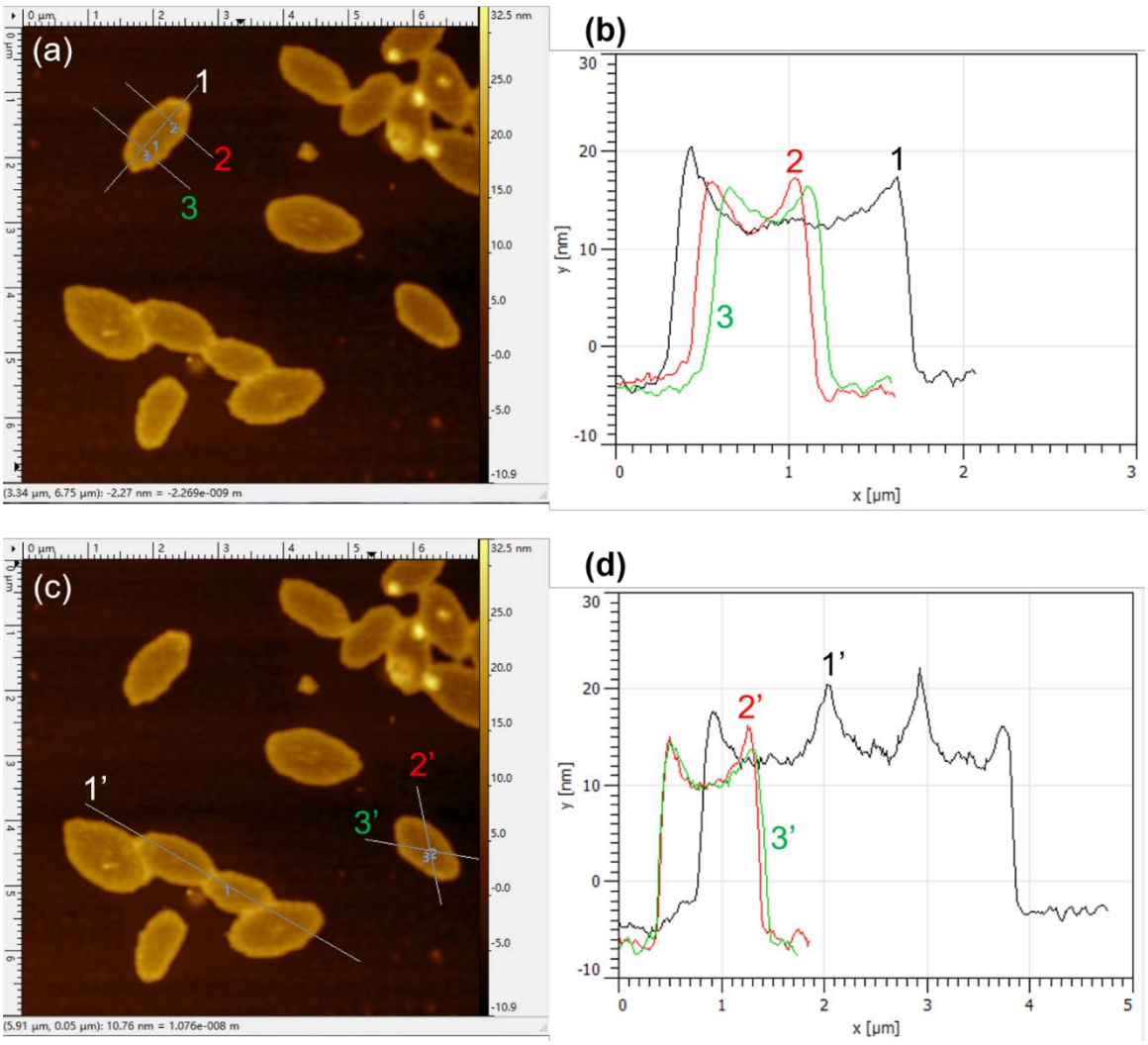

Fig. S13. (a) (c) AFM images and corresponding (b) (d) height profiles of oval micelles formed by direct self-assembly of PFS_{27}-*b*-P($TDMA_{65}$-*ran*-$OEGMA_{69}$) at 0.5 mg/mL and 80 °C in a 1:1 octane/hexanol mixture. This is the same sample for which TEM images are presented in Fig. 5 in the main text. The AFM image shows the uniformity of the structures, and the height profiles show that the ovals are higher at the edges than in the center.

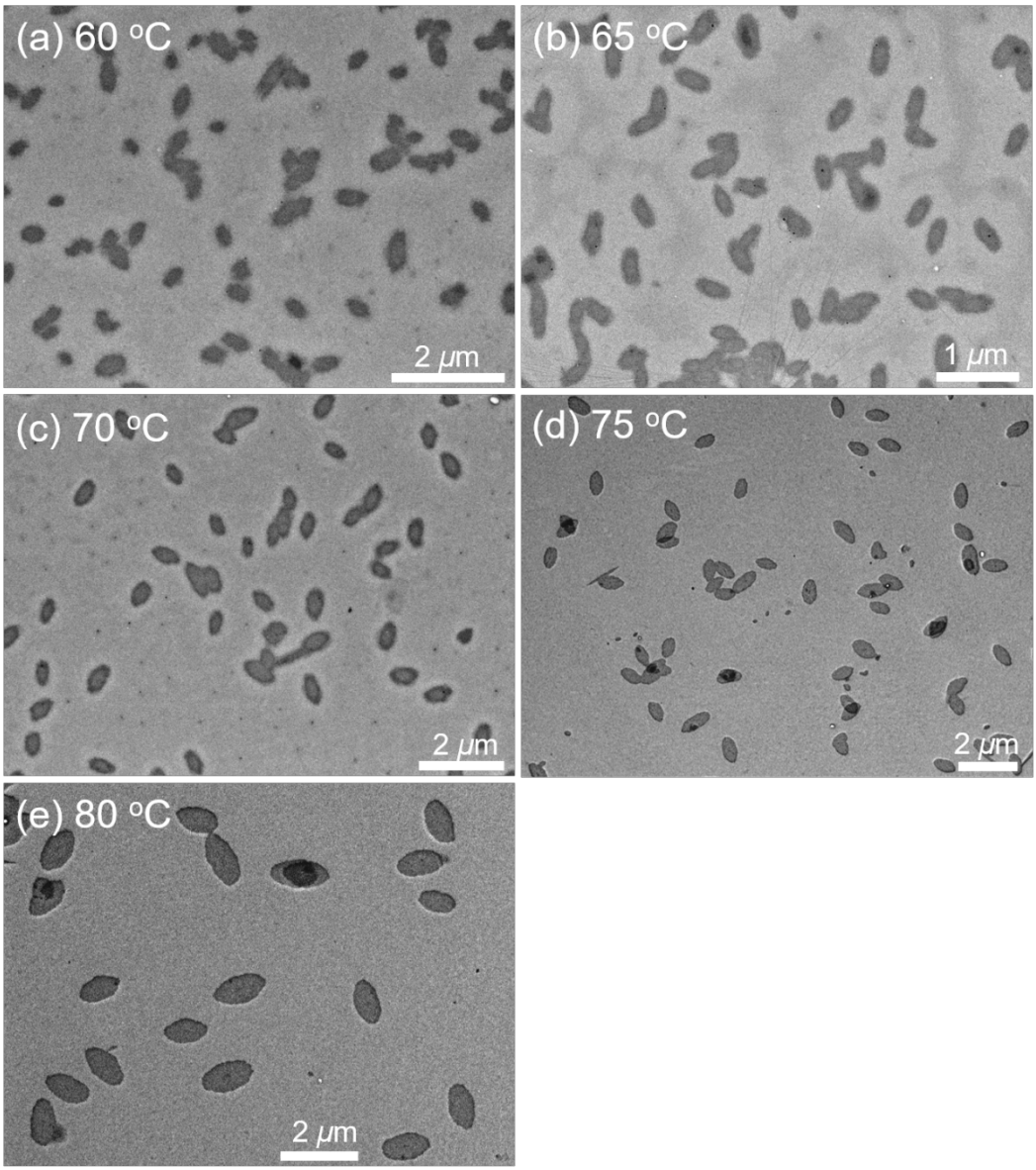

Fig. S14. Oval micelles formed by direct self-assembly at various temperatures of PFS_{27}-*b*-P($TDMA_{65}$-*ran*-$OEGMA_{69}$) at 0.5 mg/mL in a 1:1 octane/hexanol mixture. (a) 60 °C. (b) 65 °C. (c) 70 °C. (d) 75 °C. (e) 80 °C. The lengths and areas were collected in Table S1. The oval-like micelles become larger and more regular with increasingly temperature.

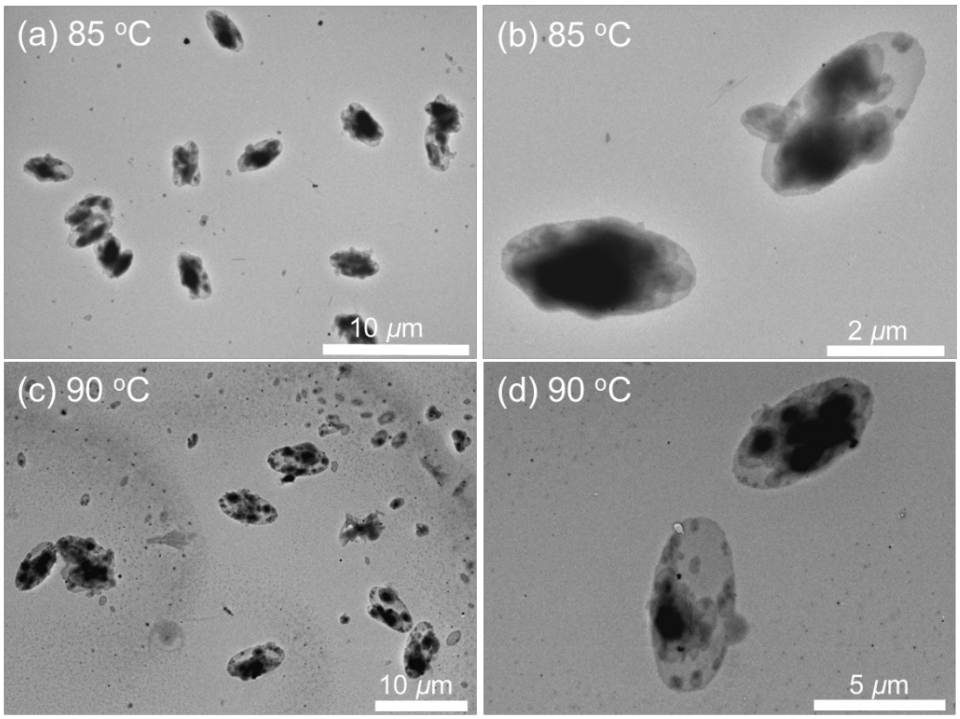

Fig. S15. Micelles formed by direct self-assembly of PFS_{27}-*b*-P($TDMA_{65}$-*ran*-$OEGMA_{69}$) at 0.5 mg/mL in a 1:1 octane/hexanol mixture at higher temperatures than the structures shown in Fig. S14. The micelles have an overall oval shape that it relatively uniform in size. (a)(b) 85 °C. (c)(d) 90 °C. (b) (d) Higher-magnification images of the structures formed. The measured lengths and areas are collected in Table S1. There are many secondary structures on the bigger oval micelles, and the micelle structure becomes more complex when prepared at higher temperature.

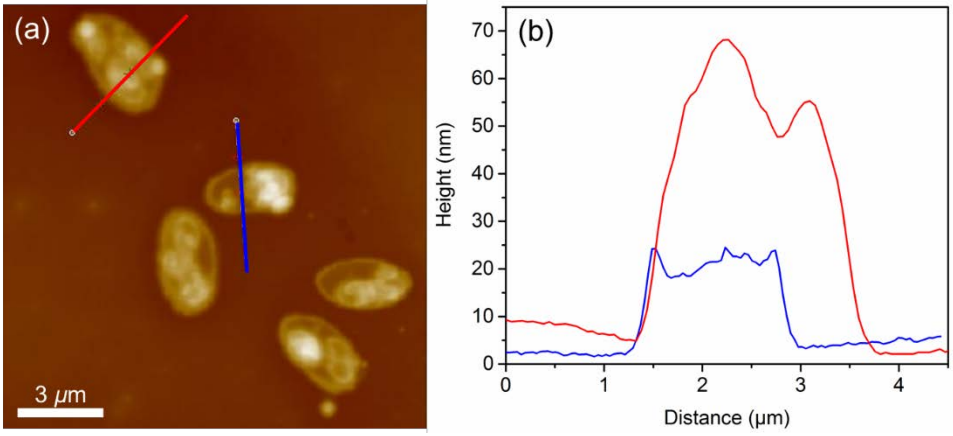

Fig. S16. (a) AFM height image and (b) height profiles of some of the oval micelles formed at 85 °C in 1:1 octane/hexanol from the same sample presented in Fig. S15. The red line and the blue line indicate that the secondary structure has grown on part of the face of the oval micelles and is nearly 70 nm high.

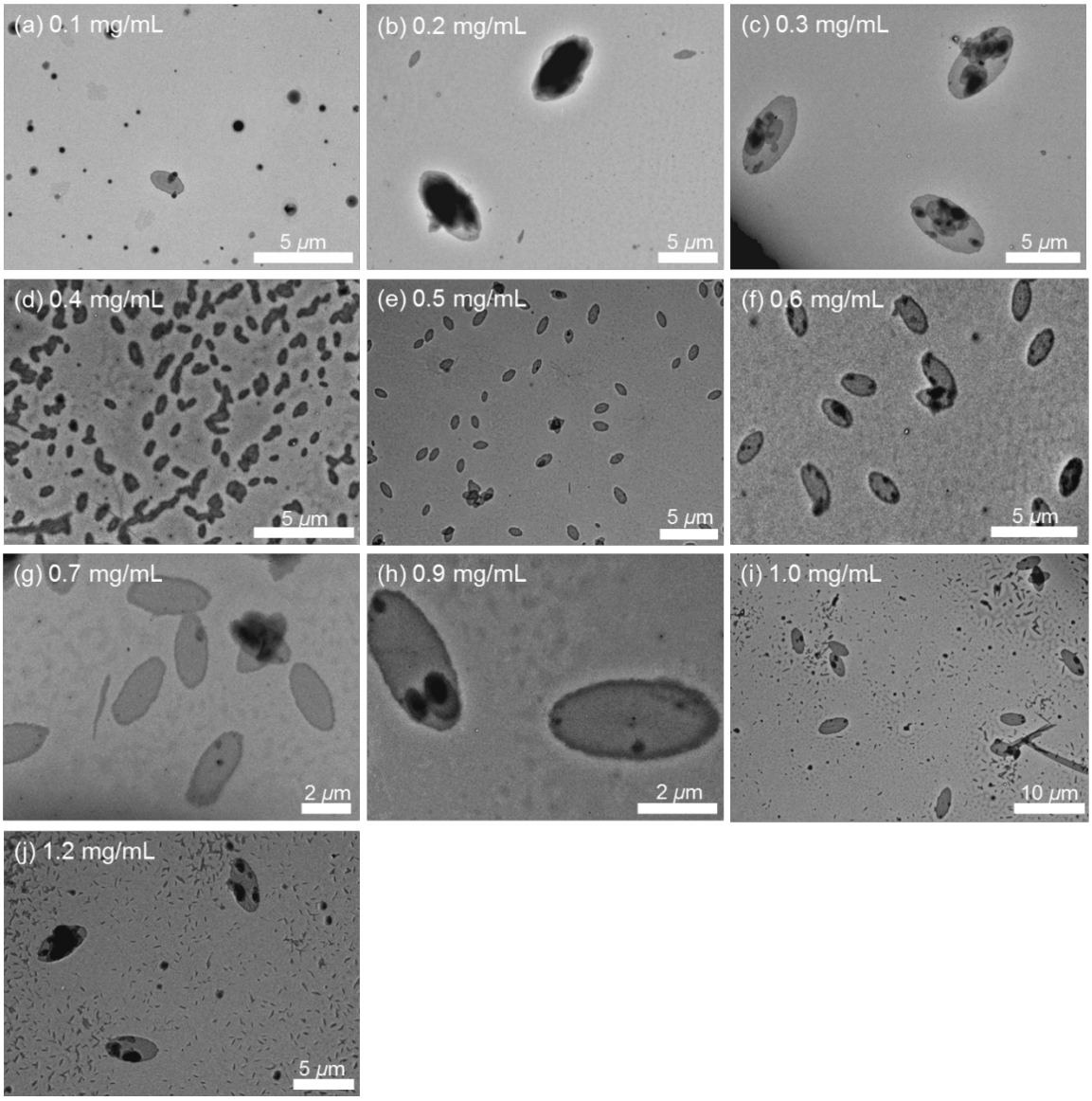

Fig. S17. Oval micelles formed by direct self-assembly of PFS_{27}-*b*-P($TDMA_{65}$-*ran*-$OEGMA_{69}$) at various concentrations in a 1:1 octane/hexanol mixture. (a) 0.1 mg/mL, few oval structures were observed. (b) 0.2 mg/mL. (c) 0.3 mg/mL. (d) 0.4 mg/mL. (e) 0.5 mg/mL. (f) 0.6 mg/mL. (g) 0.7 mg/mL. (h) 0.9 mg/mL. (i) 1.0 mg/mL, (j) 1.2 mg/mL. The measured lengths and areas are collected in Table S2. At the highest concentrations (1.0 mg/mL, 1.2 mg/mL) mixed morphologies including barbed structures (Fig. S18) were obtained.

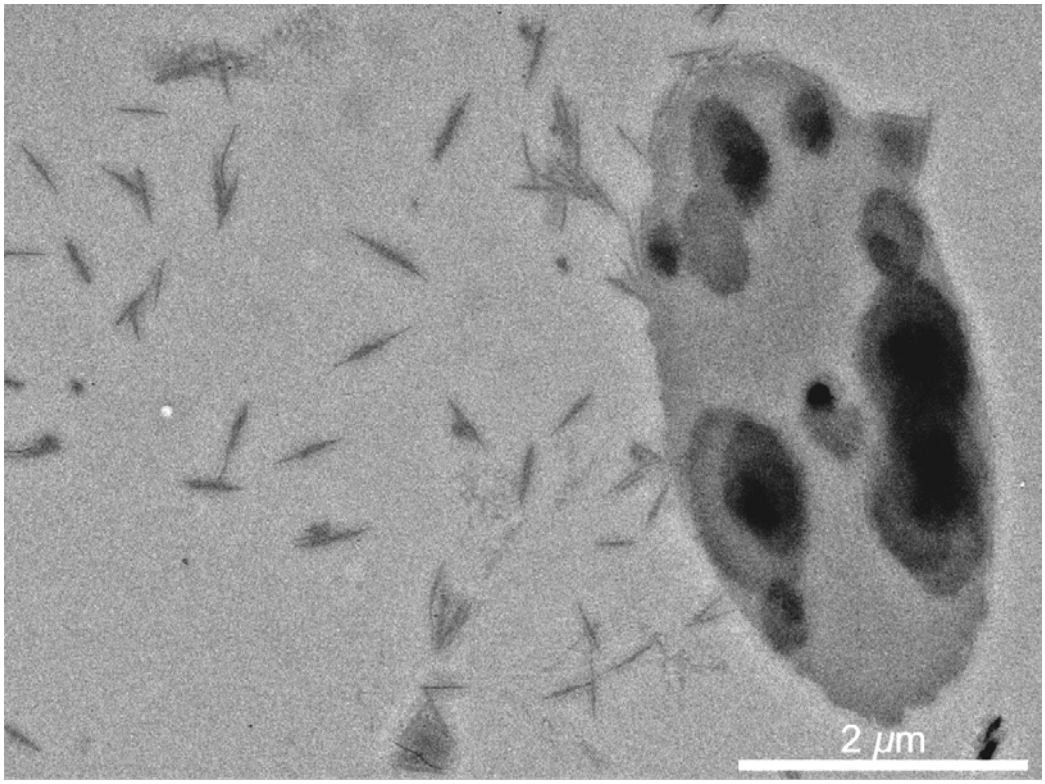

Fig. S18. High magnification image of micelles formed by direct self-assembly of PFS_{27}-*b*-P($TDMA_{65}$-*ran*-$OEGMA_{69}$) at 1.2 mg/mL in 1:1 octane/hexanol. Note the extensive secondary structure on the oval micelle and the presence of numerous fiber-like structures.

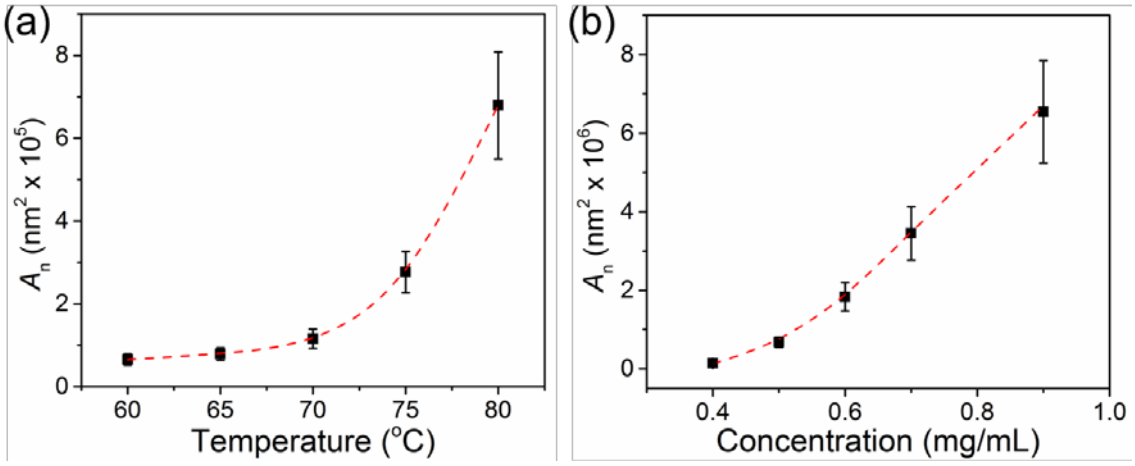

Fig. S19. Factors that affect the size (surface area A_n) of oval micelles formed by PFS_{27}-*b*-P($TDMA_{65}$-*ran*-$OEGMA_{69}$) in 1:1 octane/hexanol. Effect of (a) annealing temperature for samples at 0.5 mg/mL and (b) BCP concentration for samples heated at 80 °C for 1 h prior to cooling to RT and aging 24 h. The error bars represent the standard deviation of the area distribution.

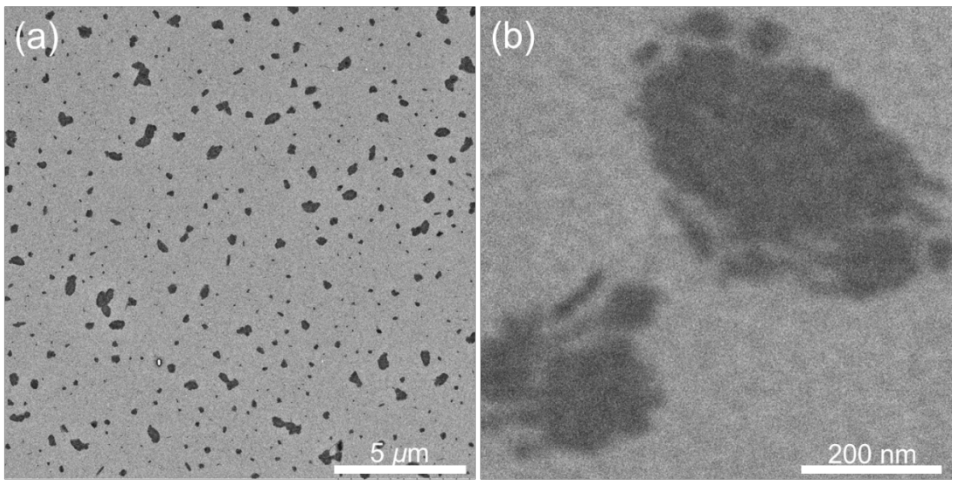

Fig. S20. Seeds after sonication of PFS_{27}-*b*-P($TDMA_{65}$-*ran*-$OEGMA_{69}$) oval micelles prepared in 1-hexanol/octane (BCP concentration 0.5 mg/mL, annealing temperature 80 °C, 1:1 (v/v)). Most of the seeds are not oval and the size is highly dispersed. The "oval" like seeds are the aggregates of many seeds as shown in (b).

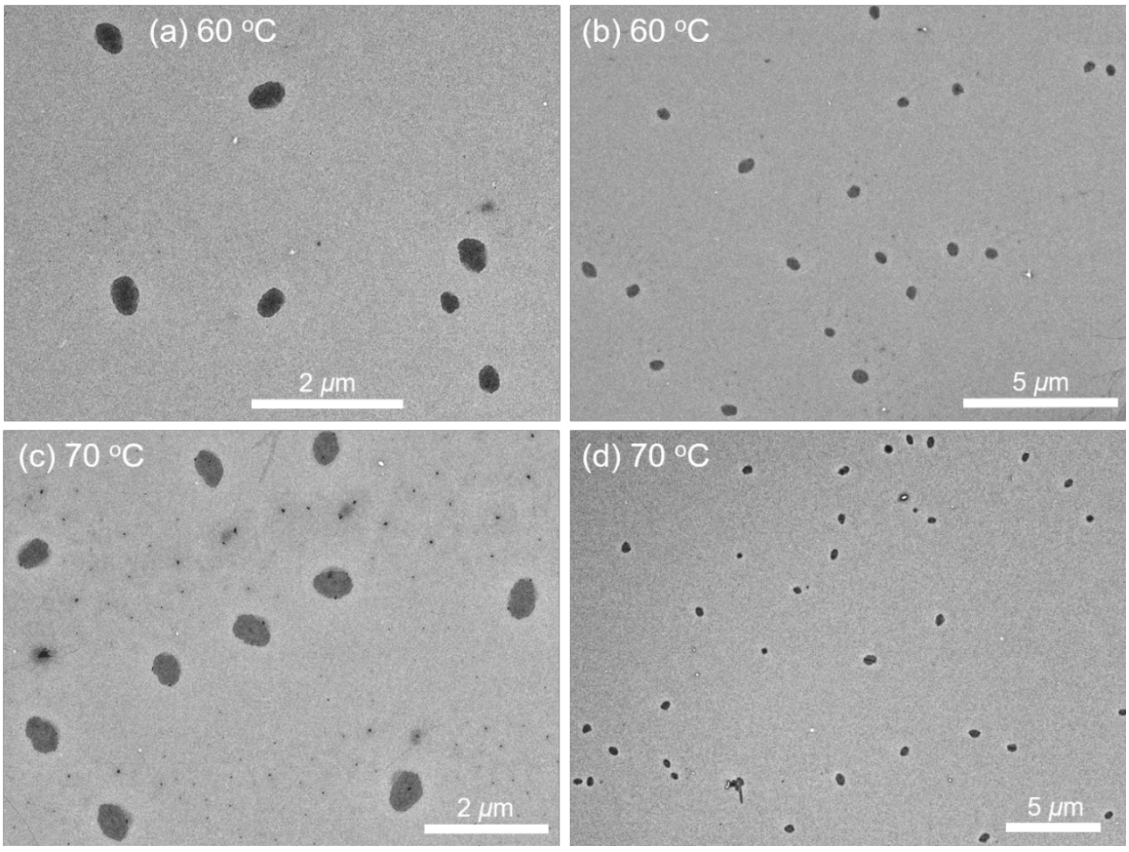

Fig. S21. Self-seeding of PFS_{27}-*b*-P($TDMA_{65}$-*ran*-$OEGMA_{69}$) oval micelles in 1-hexanol/octane (1:1 (v/v)) mixture. (a) (b) 60 °C. The oval long axis a_n = 450 nm, a_w = 473 nm, a_w/a_n = 1.05. Short axis b_n = 293 nm, b_w = 304 nm, b_w/b_n = 1.04. (c) (d) 70 °C. The oval long axis a_n = 592 nm, a_w = 606 nm, a_w/a_n = 1.02. Short axis b_n = 358 nm, b_w = 365 nm, b_w/b_n = 1.02. (b) (d) Lower-magnification images of the structures formed.

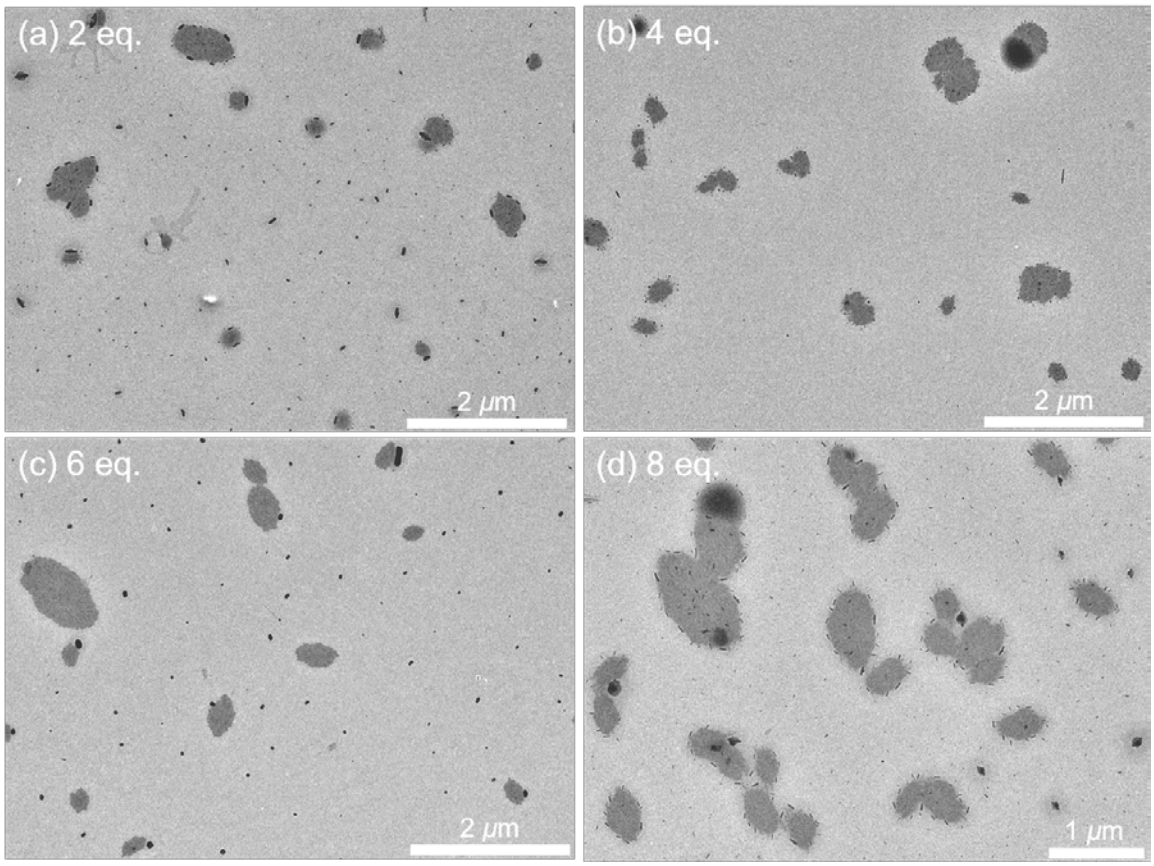

Fig. S22. Seeded growth using fragmented micelles as seeds for PFS_{27}-*b*-P($TDMA_{65}$-*ran*-$OEGMA_{69}$) oval micelles in 1-hexanol/octane (1:1 (v/v)) at different m_{unimer}/m_{seeds} ratio (eq. refers to equivalent), (a) 2 eq., (b) 4eq., (c) 6 eq., (d) 8 eq.. The broad size distribution of the structures formed by seeded growth is likely a consequence of the polydisperse nature of the seeds formed by fragmentation.

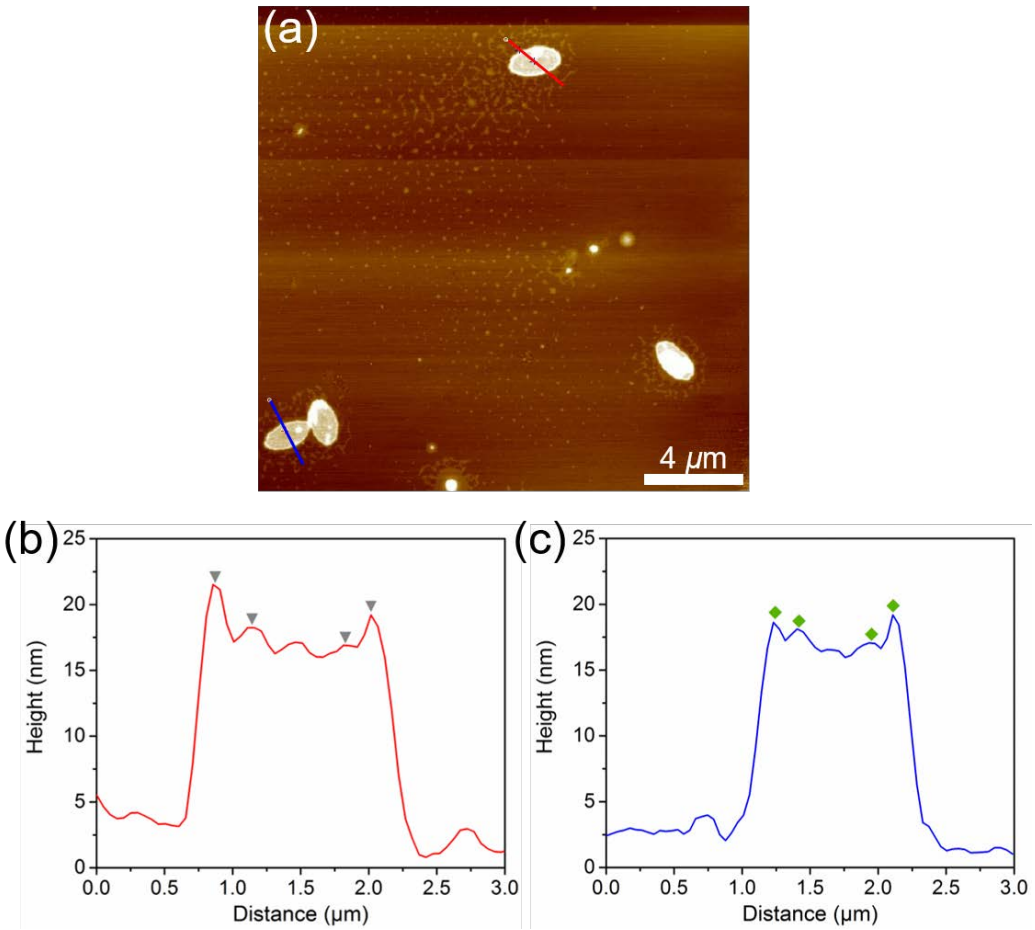

Fig. S23. Larger oval micelles obtained by seeded growth using oval micelles formed by PFS_{27}-*b*-P($TDMA_{65}$-*ran*-$OEGMA_{69}$) in 1:1 octane/hexanol at 0.5 mg/mL and 80 °C as seeds [a_n = 1249 nm (a_w/a_n = 1.01), b_n = 683 nm (b_w/b_n = 1.01), A_n = 679,440 nm^2 (A_w/A_n = 1.02)]. The unimer was added as a solution in THF (10 mg/mL) so that m_{unimer}/m_{seed} =1. (a) AFM image showing 4 micelles, (b) (c) height profiles two of these micelles. The overall height is close to 17 nm, and higher at the edges. The triangles in (b) and the diamonds in (c) appear to mark the edges corresponding to the interface between the 'seed' oval and the newly grown perimeter.

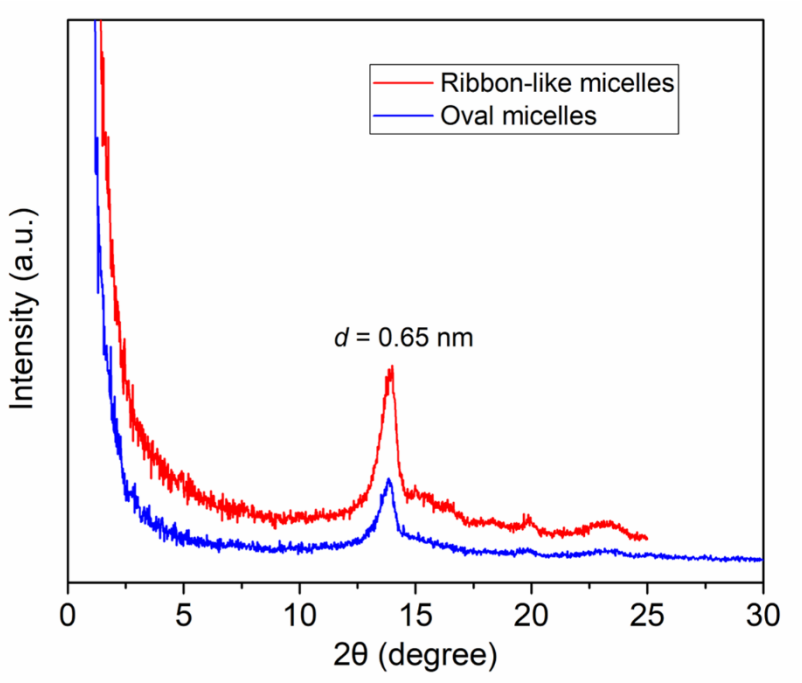

Fig. S24. X-ray diffraction (XRD) patterns obtained for ribbon-like micelles of PFS_{27}-*b*-P($TDMA_{65}$-*ran*-$OEGMA_{69}$) obtained in iPrOH (red line) and the oval micelles obtained in1:1 octane/hexanol (blue line) at 0.5 mg/mL and 80 °C respectively.

6. Supporting Tables

Table S1. Size of oval micelles formed by direct self-assembly of PFS_{27}-*b*-P($TDMA_{65}$-*ran*-$OEGMA_{69}$) at various temperatures in 1:1 (v/v) octane/hexanol. [a]

Temperature (°C)	Long axis a_n/nm (a_w/a_n)	Short axis b_n/nm (b_w/b_n)	Area A_n/nm^2 (A_w/A_n)
60	388 (1.04)	222 (1.05)	65,310 (1.03)
65	424 (1.02)	237 (1.03)	78,900 (1.03)
70	528 (1.02)	280 (1.01)	115,400 (1.02)
75	804 (1.01)	438 (1.01)	276,700 (1.04)
80	1249 (1.01)	683 (1.01)	679,440 (1.02)
85 [b]	3001 (1.01)	1499 (1.01)	3,510,200 (1.01)
90 [b]	6196 (1.003)	3103 (1.004)	14,969,700 (1.01)

[a] Self-assembly conditions: BCP concentration, 0.5 mg/mL; Heated at the temperature indicated for 1 h and then cooled to RT, then aged for 24 h.

[b] Size from the bigger oval micelles.

Table S2. Size of oval micelles formed by direct self-assembly of PFS_{27}-*b*-P($TDMA_{65}$-*ran*-$OEGMA_{69}$) at various concentrations in 1:1 (v/v) octane/hexanol. [a]

Concentration (mg/mL)	Long axis a_n/nm (a_w/a_n)	Short axis b_n/nm (b_w/b_n)	Area A_n/nm^2 (A_w/A_n)
0.1 [b]	-	-	-
0.2 [c]	6873 (1.01)	3240 (1.01)	17,360,900 (1.03)
0.3 [c]	5713 (1.02)	2940 (1.02)	13,115,400 (1.05)
0.4	582 (1.02)	308 (1.02)	136,870 (1.04)
0.5	1249 (1.01)	683 (1.01)	679,440 (1.02)
0.6	2111 (1.01)	1083 (1.01)	1,834,300 (1.03)
0.7	3046 (1.01)	1442 (1.02)	3,448,750 (1.05)
0.9	4279 (1.01)	2005 (1.01)	6,545,100 (1.01)
1.0 [c]	4244 (1.01)	2084 (1.01)	6,870,930 (1.02)
1.2 [c]	4580 (1.02)	2190 (1.02)	7,783,600 (1.03)

[a] Self-assembly conditions: heated at 80 °C for 1 h and then cooled to RT, then aged for 24 h.

[b] Few oval structures were observed.

[c] Size from the bigger oval micelles.

Table S3. Size of oval micelles by "seeded growth" using intact ovals as seeds in 1:1 (v/v) octane/hexanol.[a]

m_{unimer}/m_{seed} [b]	Long axis a_n/nm (a_w/a_n)	Short axis b_n/nm (b_w/b_n)	Area A_n/nm^2 (A_w/A_n)
0 [c]	1249 (1.01)	683 (1.01)	679,440 (1.02)
1	1715 (1.01)	957 (1.01)	1,289,700 (1.03)
2	2279 (1.01)	1202 (1.01)	2,035,200 (1.02)
3	2643 (1.01)	1415 (1.01)	2,824,200 (1.01)
5	3074 (1.02)	1653 (1.02)	3,969,700 (1.04)

[a] Self-assembly condition: oval seeds concentration, 0.05 mg/mL; unimer concentration, 10 mg/mL; RT, aged for 7 days.

[b] Mass of unimer added compared to the mass of seed micelles present.

[c] Refers to the original intact oval micelles used as seeds.

7. References

1 P. J. Roth, F. D. Jochuma and P. Theato, *Soft Matter*, 2011, **7**, 2484–2492.

2 M. Zhang, P. A. Rupar, C. Feng, K. Lin, D. J. Lunn, A. Oliver, A. Nunns, G. R. Whittell, I. Manners and M. A. Winnik, *Macromolecules*, 2013, **46**, 1296–1304.

3 H. Zhou, Y. Lu, Q. Yu, I. Manners and M. A. Winnik, *ACS Macro Lett.*, 2018, **7**, 166−171.

4 F. R. Mayo and F. M. Lewis, *J. Am. Chem. Soc.*, 1944, **66**, 1594-1601.

5 G. Moad, E, Rizzardo and S. H. Thang, *Polymer*, 2008, **49**, 1079–1131.